European Journal of Neuroscience, Vol. 25, pp. 87–98, 2007 doi:10.1111/j.1460-9568.2006.05249.x

Impaired hippocampal plasticity and errors in cognitive performance in mice with maladaptive AChE splice site selection

Noa Farchi,[1,2] Shai Shoham,[3] Binyamin Hochner[1,4] and Hermona Soreq[2,4]
[1]Department of Neurobiology, Institute of Life Sciences, The Hebrew University of Jerusalem, Israel 91904
[2]Department of Biological Chemistry, Institute of Life Sciences, The Hebrew University of Jerusalem, Israel 91904
[3]Research Department, Herzog Hospital, Jerusalem, Israel 91351
[4]The Interdisciplinary Center for Neuronal Computation, The Hebrew University of Jerusalem, Israel 91904

Keywords: acetylcholinesterase, cognition errors, LTP, stress, transgenic mice

Abstract

Neuronal splice site selection events control multiple brain functions. Here, we report their involvement in stress-modulated hippocampal plasticity and errors of cognitive performance. Under stress, alternative splicing changes priority from synaptic acetylcholinesterase (AChE-S) to the normally rare, soluble and monomeric AChE-R variant, which facilitates hippocampal long-term potentiation (LTP) and intensifies fear-motivated learning. To explore the adaptive value of changes in AChE splicing, we compared hippocampal plasticity and errors of executive function in TgS and TgR transgenic mice overexpressing AChE-S or AChE-R, respectively. Hippocampal slices from TgS and TgR mice presented delayed and facilitated transition to LTP maintenance, respectively, compared with strain-matched FVB/N controls. TgS slices further showed failed recruitment of both the α-amino-3-hydroxy-5-methylisoxazole-4-propionate and *N*-methyl-D-aspartate components of LTP, refractory response to cholinergic enhancement and suppressed protein kinase C (PKC) levels. Stable LTP could, however, be rescued by phorbol ester priming, attributing the TgS deficits to disrupted signal transduction. In serial maze tests, TgS mice displayed more errors of conflict and executive function than did FVB/N controls, reflecting maladaptive performance under chronic AChE-S overexpression. In contrast, TgR mice displayed enhanced serial maze performance, suggesting that chronic AChE-R overexpression facilitates adaptive reactions. Our findings are compatible with the notion that changes in the alternative splicing of AChE pre-mRNA and consequent alterations in PKC signalling are causally involved in modulating hippocampal plasticity and cognitive performance.

Introduction

Alternative splicing of pre-mRNA may be viewed as a beneficial adaptation strategy, which modifies a finely tuned regulation process yet might induce adverse consequences (Meshorer & Soreq, 2002). This is particularly apparent for mammalian stress responses, which involve regulated, specific modulations in neuronal alternative splicing (Shin & Manley, 2004). Supporting this notion, splicing aberrations were reported in many diseases (Stoilov *et al*., 2002), such as fronto-temporal dementia with parkinsonism (Stamm *et al*., 2005), as well as in ageing (Meshorer *et al*., 2002). However, the relevance of alternative splicing to the stress-associated interference with hippocampal plasticity and errors in cognitive performance of otherwise healthy subjects, as well as the molecular mechanism(s) involved, remain largely obscure.

Stress may improve or disrupt cognition at different levels of function. At the behavioural level, stress can impair learning and performance (Diamond *et al*., 1999) or enhance it (Blank *et al*., 2002). It was suggested that the mechanisms underlying these robust effects may involve stress-dependent modulation of hippocampal synaptic plasticity (Kim & Diamond, 2002). Indeed, stress can enhance or disrupt hippocampal long-term potentiation (LTP) (Sapolsky, 2003). *In vitro* and *in vivo* studies demonstrate both stress-induced impairment of high-frequency stimulation (HFS) LTP (Foy *et al*., 1987; Shors *et al*., 1989) and stress-induced facilitation of theta burst stimulation (TBS) LTP at CA1 synapses (Blank *et al*., 2002). Correlative studies in humans suggest that activation of the hypothalamic-pituitary axis contributes to errors of cognition (al'Absi *et al*., 2002).

Cholinergic pathways contribute to both stress and cognitive functions. Thus, cholinergic neurons are activated in response to stress (Kaufer *et al*., 1998; Meshorer & Soreq, 2002; Meshorer *et al*., 2002), and nicotine enhances cognitive performance (Maskos *et al*., 2005). The cingulate cortex, prefrontal cortex and hippocampus receive extensive cholinergic innervation, and are implicated both in cognitive control of executive function and in error monitoring (Carter *et al*., 1998). The underlying synaptic mechanism(s) may modulate associative processes by interfering with acetylcholine (ACh) enhancement of LTP (Hirotsu *et al*., 1989; Blitzer *et al*., 1990; Sokolov & Kleschevnikov, 1995). An additional possibility, however, is that non-catalytic properties of acetylcholinesterase (AChE) are involved (Soreq & Seidman, 2001). AChE pre-mRNA shows modified alternative splicing under stress (Meshorer & Soreq, 2006), and is therefore a prime candidate mediator for stress-induced modulation of the non-catalytic AChE properties and, suggestively,

Correspondence: Dr H. Soreq, as above.
E-mail: soreq@cc.huji.ac.il

Received 28 June 2006, revised 26 September2006, accepted 25 October 2006

of hippocampal function. Under normal conditions, the primary 'synaptic' (Perrier *et al*., 2005) variant AChE-S dominates, but under stress, alternative splicing elevates the normally rare 'readthrough' AChE-R variant. Unlike AChE-S, which adheres to membranes in a tetrameric structure, AChE-R is a soluble monomer. Because AChE-R also terminates cholinergic neurotransmission, the adaptive value for cognition of this shift remained unclear. This concept could be challenged, however, in mice overexpressing either of the AChE variants, where transgenic AChE-R excess would overshadow intrinsic AChE-S and vice versa. We have previously shown that TgR mice overexpressing AChE-R display exaggerated contextual fear-induced behavioural inhibition (Birikh *et al*., 2003) and intensified synaptic plasticity (Nijholt *et al*., 2004). In contrast, TgS mice with AChE-S overexpression display increased accumulation of ageing-associated neuronal stress hallmarks (Sternfeld *et al*., 2000), spatial learning deficits (Beeri *et al*., 1997) and massive alterations in neuronal gene expression (Meshorer *et al*., 2005a).

Here, we measured LTP analyses and corresponding pharmaceutical interventions in hippocampal slices. At the cognitive level, we explored the effects of increased AChE-R or AChE-S accumulation on a learning task not involving fear. Our findings demonstrate an inverse phenotype for TgS as compared with TgR mice, both in neuronal plasticity and in performance errors, suggesting active contribution of maladaptive splice site selection to stress-induced cognitive malfunctioning.

Materials and methods

Slice preparation and electrophysiology

Hippocampal slices were obtained from 3–6-month-old, male and female mice with the experimenter blind to the group identity (FVB/N, TgS or TgR mice or transgenic AChE-Sin mice overexpressing catalytically inactive AChE-Sin; Trullas & Skolnick, 1993; Dori *et al*., 2005). Transgenic lines were all developed from inbred FVB/N mice (Royle *et al*., 1999; Mineur & Crusio, 2002). Animal treatment, use and mode of death were reviewed and approved by the Hebrew University Committee for Animal Experimentation. Animals were killed by cervical dislocation; brains were rapidly removed and placed in ice-cold artificial cerebrospinal fluid (ACSF) consisting of (in mM): NaCl, 124; KCl, 5; $NaHCO_3$, 26; NaH_2PO_4, 1.2; $MgSO_4$, 1.3; $CaCl_2$, 2.4; glucose, 10 (gassed with 95% O_2/5% CO_2). Transverse slices (400 μm) were prepared from isolated hippocampus by standard techniques and incubated at room temperature for at least 1.5 h before recording. During recording in the chamber, slices were perfused continuously (2 mL/min) with warm (32 °C) ACSF. One pole of a bipolar, stainless steel stimulating electrode, placed in the stratum radiatum of the CA1 region of the slice, was used to activate the Schaffer collaterals. Extracellular recording of field potentials was performed with an ACSF-filled glass microelectrode (3–6 MΩ) placed in the stratum radiatum of the CA1 area. A test pulse of 0.05 ms duration was delivered at 0.033 Hz and was set to evoke baseline field excitatory postsynaptic potentials (fEPSPs) reaching ~50% of the maximal fEPSP slope. Control recordings were taken for 20 min, followed by LTP induction by one of two tetanization protocols: HFS consisted of three trains of 1 s duration at a frequency of 50 Hz with a 20-s intertrain interval, and pulse duration doubled to 0.1 ms in the tetanus. TBS consisted of five trains of five 0.05 ms duration pulses, at a frequency of 100 Hz and with a 200-ms intertrain interval. Following LTP induction, fEPSPs were recorded from at least 60 min and up to 180 min.

Data acquisition and analysis were performed with LabView software (National Instrument, Austin, TX, USA). fEPSP slopes were measured and normalized to average values of the control period. All values are reported as mean ± SEM of all slices tested in the corresponding paradigm, with each value representing a mean of 10 data points. Statistical comparisons were based on unpaired Student's *t*-tests.

In situ *hybridization*

Coronal brain slices (7 μm) were hybridized as described earlier (Meshorer *et al*., 2005a), with a 50-mer digoxigenin-labelled 2-O-methylated antisense cRNA probe (Microsynth, Balgach, Switzerland) complementary to exon six of the *ACHE* gene. Probe detection was with a streptavidin-alkaline phosphatase conjugate (Amersham Pharmacia Biotech, Little Chalfont, UK) and Fast Red as the reaction substrate (Roche Diagnostics, Mannheim, Germany). Micrographs of the hippocampal area were subjected to qualitative evaluation of Fast Red staining intensity.

Protein immunoblot analyses

Protein samples from intact mouse hippocampi, prepared in ice-cold low-salt detergent buffer (phosphate-buffered saline, 0.1% Triton X-100 and 0.02 mg/mL each of aprotinin, leupeptin and pepstatin) were cleared by centrifugation and were subjected to a protein quantification assay (Lowry assay, Bio-Rad, Hercules, CA, USA). Fifteen micrograms of total protein samples were separated by sodium dodecyl sulphate–polyacrylamide gel electrophoresis, and electroblotted onto a nitrocellulose membrane (Bio-Rad). Membranes were blocked with Ponceau reagent (Sigma, St. Louis, MO, USA) for comparison of total protein loads on gels. Only membranes with comparable lane-staining were processed for antibody detection. Membranes were blocked in Tris buffer saline (10 mM Tris-Cl, pH 8.0, 150 mM NaCl, 0.05% Tween 20) with 5% non-fat dry milk powder (Bio-Rad) for 1 h at room temperature, and then incubated with primary antibody (4 °C, overnight). Following washes with Tris buffer saline (3 × 10 min), membranes were incubated with appropriate horseradish peroxidase-conjugated secondary antibody in blocking solution (room temp, 2 h), washed as above and bound antibodies were visualized with an ECL kit (Amersham Biosciences, Buckinghamshire, UK). Antibodies used were rabbit anti-mouse PKCβII (1 : 8000, Sigma) and donkey anti-rabbit as secondary antibody (1 : 10,000, Sigma).

AChE activity measurements

Acetylthiocholine hydrolysis levels were determined following hippocampal homogenization, as described (Ellman *et al*., 1961). Briefly, homogenates (10 μL) were added to a reaction mix (0.2 mL total volume) containing (in mM): Na_2HPO_4, 80; acetylthiocholine iodide, 0.63; 5,5′-dithio-bis (2-nitrobenzoic acid) (Ellman's reagent), 0.5; and tetraisopropyl pyrophosphoramide (iso-OMPA, butyrylcholinesterase inhibitor), 0.1. Production of the yellow nitrobenzoate anion was measured at 412 nm by means of a multiwell plate reader (Tecan, Maennedorf, Switzerland).

Materials

Carbachol, physostigmine, forskolin and phorbol dibutyrate (PDBu) were purchased from Sigma. Both forskolin and PDBu were prepared as concentrated stock solutions in dimethylsulphoxide (DMSO) and then diluted into ACSF before each experiment (maximal final DMSO concentration, 0.1%).

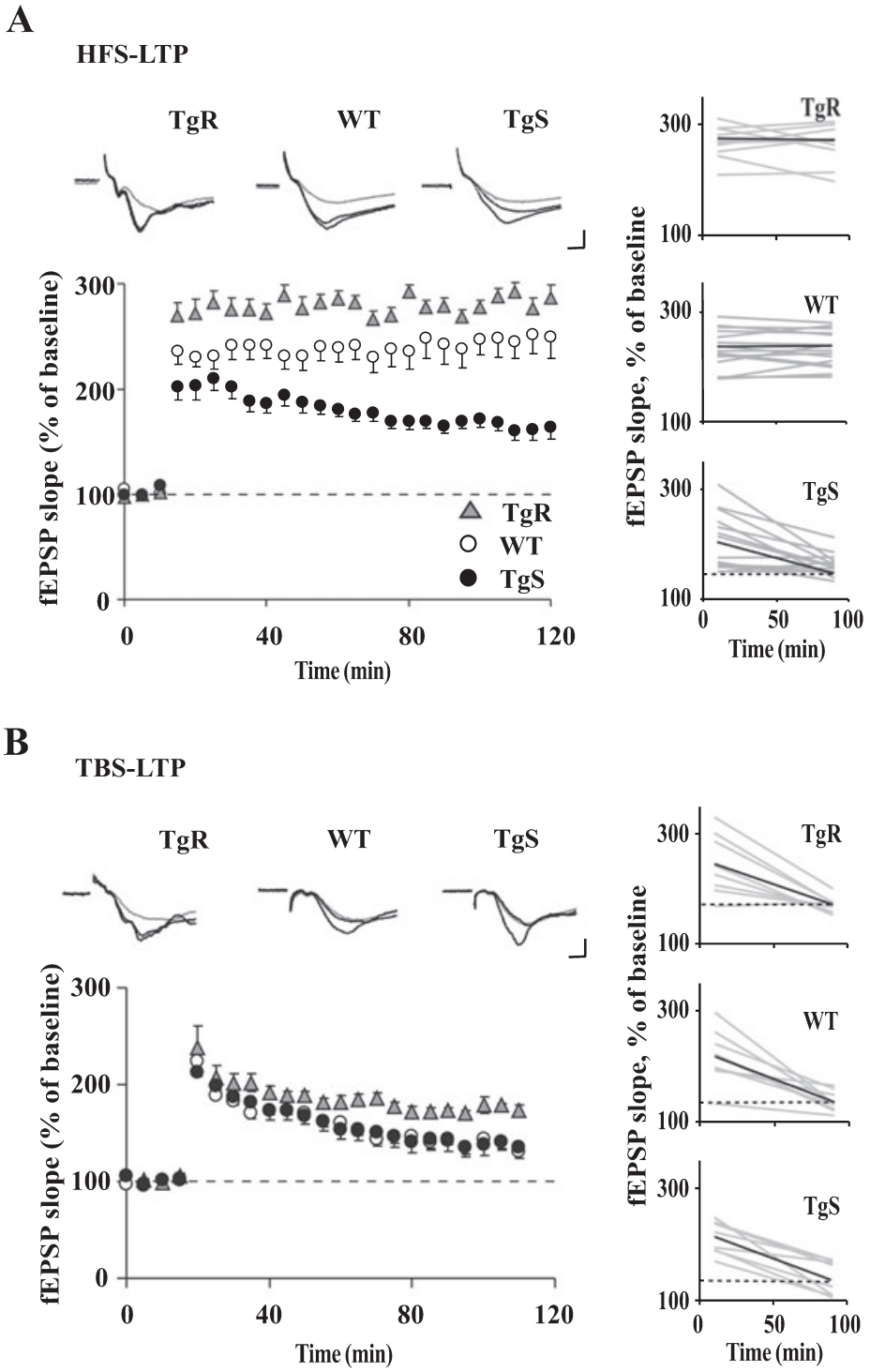

FIG. 1. Long-term potentiation (LTP) maintenance is impaired under inherited excess of AChE-S but not AChE-R. Schaffer collaterals–CA1 synapses were stimulated to induce LTP. (A) High-frequency stimulation (HFS)–LTP. Insets are averaged sampled baseline (grey line), 10′ and 90′ post-tetanus (black lines) field excitatory postsynaptic potentials (fEPSPs) from TgR, wild-type (WT) and TgS slices. Scales: 0.5 mV, 5 ms. Shown below are averaged analyses of hippocampal slices from the three mouse lines under HFS applied after 15–20 min of baseline recordings. Right panel, individual analyses of decaying slopes from 10 to 90 min post-HFS. The majority of hippocampal slices from TgS (bottom) display LTP decay as compared with TgR (top) and WT (middle). Averaged decays are marked by black lines. (B) Theta burst stimulation (TBS)–LTP. Similar analyses as in (A) of potentiation responses but with TBS of slices from the three mouse lines (bottom). Indifferent to the stimulation protocol, TgR slices consistently present facilitated, stable potentiation, whereas TgS slices display decayed potentiation.

Two-unit linear serial choice maze

This maze is made of modular units placed in a series (Quartermain *et al*., 1994). In each unit, a mouse must choose between turning right and left. At the end of the maze the mouse receives a reward in the form of 40 μL of sweetened water (5% sucrose), and one 'run' is considered complete. Then the mouse must shuttle back to the other end of the maze where it gets the same reward. Wall

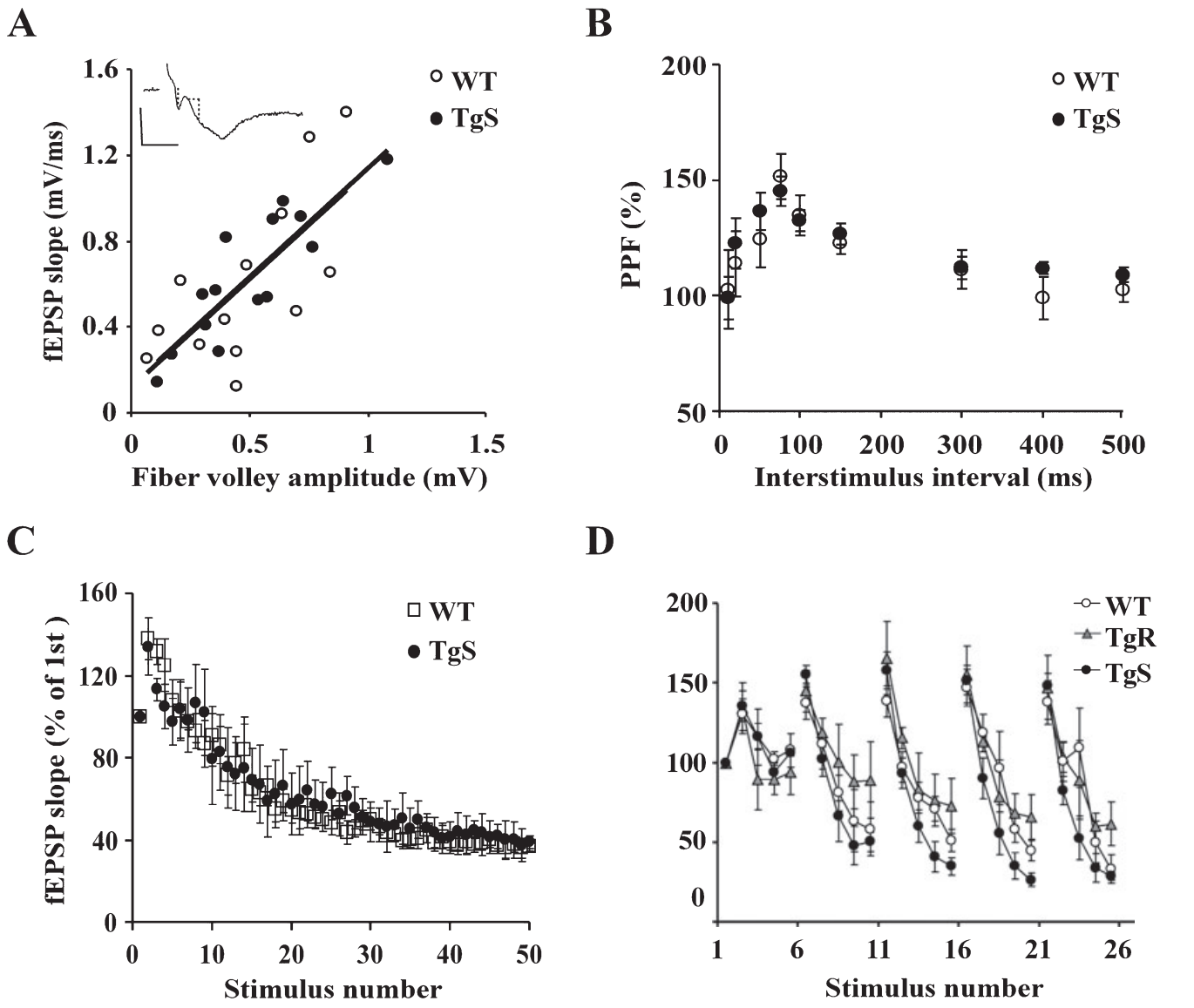

FIG. 2. Inherited excess of AChE-S does not affect transmission properties. (A) Excess AChE-S had no effect on the excitability of Schaffer collaterals–CA1 synaptic connections. Shown are analyses of field excitatory postsynaptic potential (fEPSP) slopes elicited by three stimulation intensities, quantified by the fibre volley amplitude ($n = 4$ mice of each strain). The inset trace displays measured variables, scale 0.5 mV, 1.5 ms. Regression slopes were: for TgS $= -1.01$/ms ($R^2 = 0.75$, $P < 0.001$) and for wild-type (WT) $= -1.02$/ms ($R^2 = 0.5$, $P < 0.008$). (B) WT and TgS slices present similar paired pulse facilitation (PPF) with the indicated interstimulus intervals. (C) WT and TgS slices show parallel dynamics of the fEPSP decay during the HFS train or (D) TBS trains of the three mouse lines. fEPSPs were normalized to the first synaptic response in the train.

partitions within the maze force the mouse to make 'right-' or 'left-'turning choices. When advancing from one end of the maze, the correct sequence is right–right, whereas in the opposite direction the correct response is left–left. The innate (prepotent) tendency of mice is to adopt a single motor sequence in both directions. Namely, to always turn right or always turn left. Inhibition of this prepotent motor response strategy requires executive function and constant monitoring of potential errors. Thus, this test is sensitive to the functional involvement of limbic brain regions, e.g. hippocampus and cingulated/prefrontal cortex that monitor competing motor decisions and thus prevent errors (Carter *et al.*, 1998; McNaughton & Wickens, 2003). Quantitative measures of performance include the number of left/right choice errors, 'retrace errors' – number of episodes in which a mouse moves in the wrong direction (toward the end of no reward), time to complete a session (five rewarded runs) and the number of errorless runs per session (five errorless runs is the highest level of performance). Statistical comparisons are based on analysis of variance with Newman–Keuls *post hoc* tests. Three–five-month-old male FVB/N, TgS or TgR mice were water deprived for 22 h and allowed five runs per session; one session per day.

The elevated plus maze

The maze was constructed as described (Trullas & Skolnick, 1993). All tests were conducted under dim illumination. The quantified parameters included the time spent in the open arms and the ratio between entries into open arms and the total number of arm entries. Both provide estimates of the conflict between the innate tendency to hide and the tendency to explore. The total number of arm entries served as an estimate of overall motor activity.

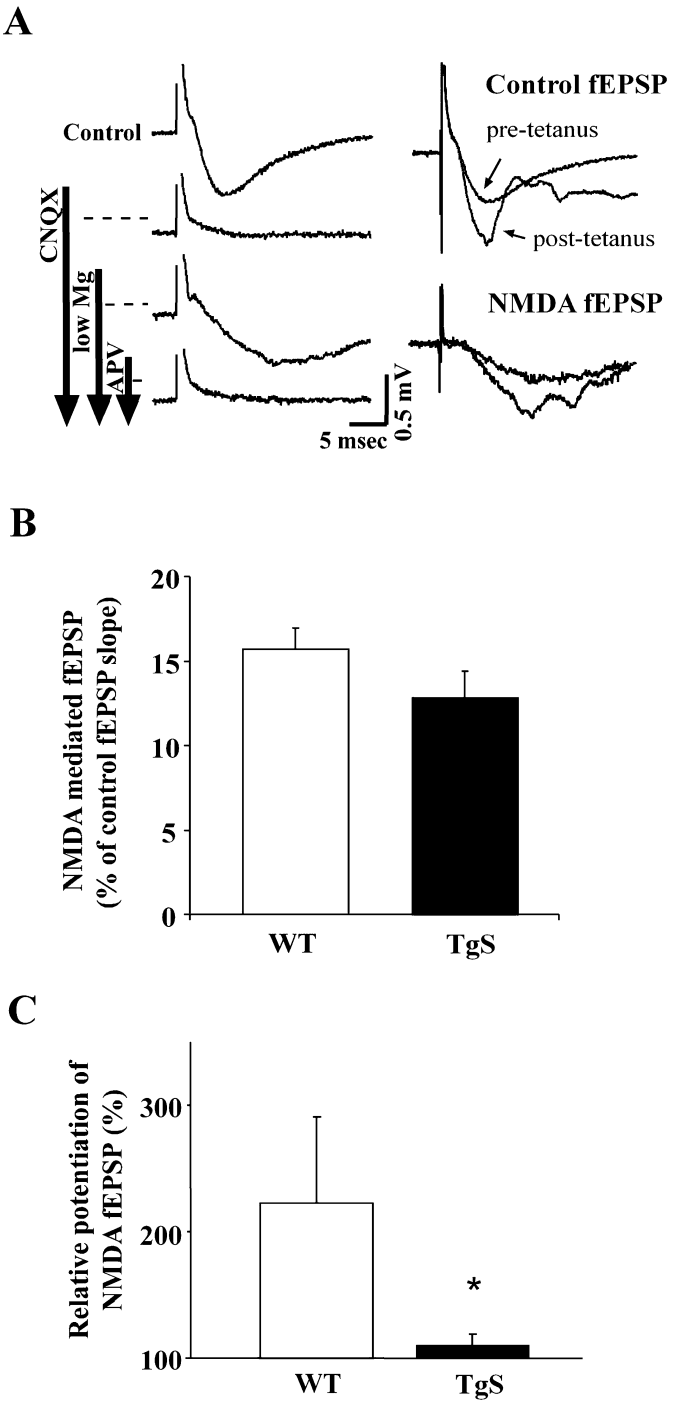

FIG. 3. Transgenic *N*-methyl-D-aspartate (NMDA)-mediated field excitatory postsynaptic potential (fEPSP) does not potentiate during L-LTP. (A) NMDA-mediated fEPSPs were determined in low Mg^{2+} (0.1 mM) and CNQX (20 μM) solution, and then controlled by blockade with APV (50 μM). (B) The NMDAR component was calculated as the ratio of between the slope of the fEPSP response in the presence of low Mg^{2+} and AMPA inhibitors and control responses. No significant differences were found between the NMDA component of wild-type (WT) and TgS responses. (C) The NMDA component was re-determined 1.5 h following LTP induction and was significantly potentiated only in WT slices but not in TgS. *$P < 0.05$ comparing WT and TgS.

Results

Stress-induced neuronal hypersensitivity involves intensified cholinergic–glutamatergic interactions (Meshorer & Soreq, 2002; Meshorer *et al*., 2002), which were demonstrated in several brain regions to affect CNS functions, such as LTP, memory and behaviour (Aigner, 1995), all subject to modulation following stress**.** To search for the involvement of AChE pre-mRNA alternative splicing with glutamatergic synaptic plasticity, LTP was measured in the CA1 region of hippocampal slices from TgS, TgR and parent strain FVB/N mice.

Overexpressed AChE-S interferes, whereas AChE-R facilitates the transition to L-LTP

Both TgS and TgR mice displayed 50–80% elevation in brain AChE activities, close to the levels reached in the stressed brain (Birikh *et al*., 2003). CA1-LTP was induced using two distinct protocols yielding post-tetanization increases, which differ in their maintenance phase. HFS induces long-lasting LTP, whereas TBS is characterized by decaying potentiation. Our previous results demonstrated a modulatory action for AChE-R in the facilitation of Schaffer collaterals–CA1 HFS–LTP (Fig. 1A, modified from Nijholt *et al*., 2004). In comparison, the potentiation response to HFS was 209 ± 16% in TgS slices ($n = 20$ slices, 16 mice), not significantly different from FVB/N slices reaching 235 ± 12% ($n = 16$ slices, 13 mice; Fig. 1A). Decay rates were calculated as the percentage reduced potentiation during 90 min post-induction, where peak potentiation was normalized to 100%. Surprisingly, fEPSP slopes decayed progressively in the TgS slices to a level of 160 ± 9% by 2 h post-tetanus at a rate of −22.8% potentiation per hour, whereas wild-type (WT) and TgR LTP sustained stable values of potentiation (Fig. 1A). These findings suggested that excess AChE-S interferes with the transition to the late phase of LTP, the inverse to AChE-R, which actively contributes to the facilitation of LTP induction and maintenance. The TBS–LTP profiles of TgS slices closely followed the decay of WT slices ($n = 10$ slices, five TgS mice, Fig. 1B). TgR-induced augmentation was also revealed using TBS–LTP (Fig. 1B), displaying slower decay of the potentiation from 237 ± 17% to 173 ± 5% in TgR as compared with 224 ± 3% to 130 ± 7% decay of WT slices at a time point of 90 min post-induction ($n = 7$ slices, four TgR mice and eight slices, four WT mice, $P < 0.05$). These findings demonstrated a possible link between the alternative splicing shift from AChE-S to AChE-R and the shift from decaying to maintained LTP.

AChE-S-induced LTP impairments occur in spite of sustained neurotransmission dynamics

To test the possibility that the decaying LTP pattern in TgS mice reflects synaptic impairments, we characterized neurotransmission dynamics. WT and TgS slices presented a similar dependence of fEPSP slopes on presynaptic fibre volley amplitudes (Fig. 2A, $n = 4$ animals each). As a measure of presynaptic function, we examined paired-pulse facilitation, a transient form of presynaptic plasticity presumably dependent on the slower kinetics of residual calcium removal at the presynaptic site (Hochner *et al*., 1991). TgS and WT slices presented comparable paired-pulse facilitation in all of the measured interstimulus intervals (Fig. 2B). Additionally, we examined the synaptic efficacy of the train composing the induction stimuli of HFS–LTP or TBS–LTP. Similar dynamic changes of fEPSP during the train were observed in TgS and WT slices under both modes of stimulation (Fig. 2C, $n = 5$ slices, five mice each). This excluded tetanization input differences as the cause of the progressive TgS decline in HFS–LTP. In a similar manner, the different HFS–LTP pattern displayed by TgR slices could not reflect differences in induction efficacy, as the first of five induction trains of TBS–LTP did not significantly differ between TgR, WT and TgS slices (Fig. 2D,

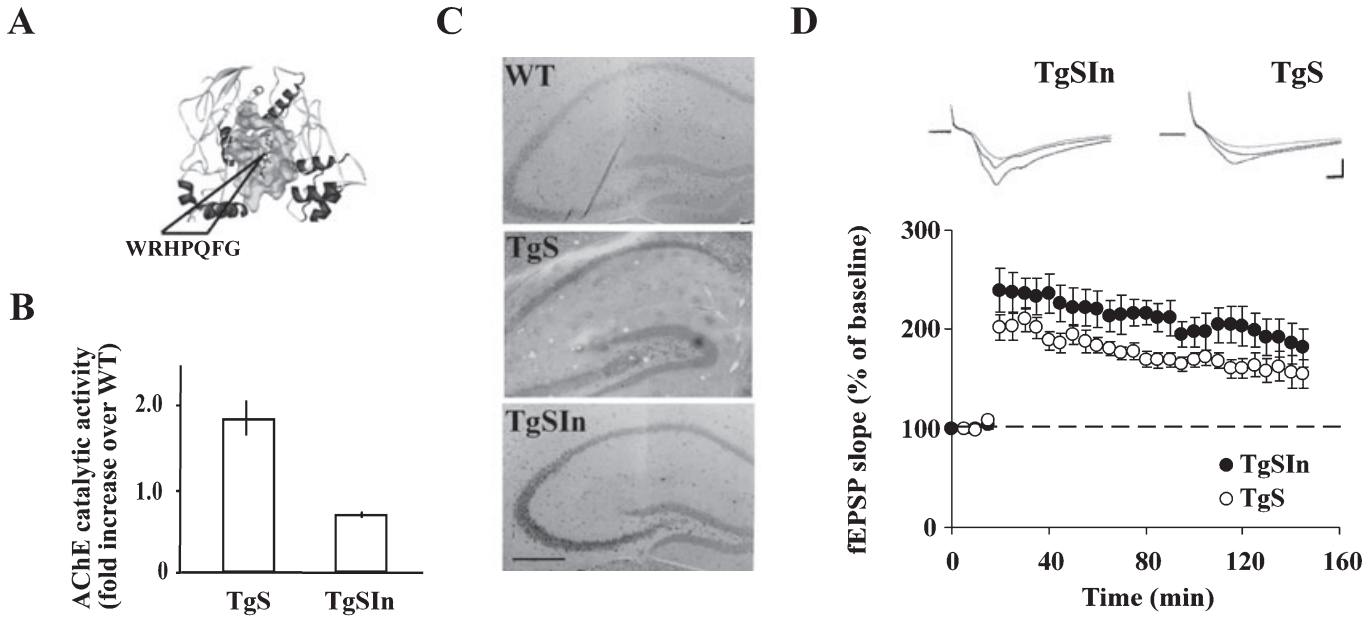

FIG. 4. Excess of inactive acetylcholinesterase (AChE)-S induces LTP decay. (A) Schematic representation on crystallographic model of AChE-S with an insert of seven amino acids at the catalytic site to create inactivated enzyme. (B) Columns present a fold increase from wild-type (WT) of ACh hydrolytic activity in hippocampal homogenates. (C) Shown are hippocampal slices from TgS (centre) and TgSIn (bottom) brains stained for AChE-S mRNA by fluorescent *in situ* hybridization in comparison to parallel sections from WT mice (top). Scale bar: 0.5 mm. Note the enhanced mRNA signals in TgSIn, albeit low AChE hydrolytic activity, indicative of the presence of the inactive enzyme. (D) Displayed are averaged sampled baseline (grey line), 10′ and 90′ post-tetanus (black lines) field excitatory postsynaptic potentials (fEPSPs) from TgSIn and TgS hippocampal slices, scales: 0.5 mV, 1.5 ms. Below, averaged analysis of TgSIn hippocampal slices as compared with TgS (replotted from Fig. 1A) in response to HFS.

$n = 7$ of each). It should be noted though that later trains already display smaller depression for TgR fEPSP than that of TgS slices. Together, these findings demonstrate that the observed failure in the LTP maintenance phase of TgS slices appeared in spite of normal basal synaptic transmission.

N-methyl-D-aspartate receptor (NMDAR)-mediated fEPSP fails to potentiate during the TgS maintenance phase

To explore whether the failure in the maintenance phase is limited to a specific glutamatergic receptor, we determined the NMDAR component in TgS LTP. fEPSPs were examined in the presence of the α-amino-3-hydroxy-5-methylisoxazole-4-propionate receptor (AMPAR) blocker CNQX (20 μM) and low Mg^{2+} concentration (0.1 mM), and were controlled by NMDAR block using APV (50 μM, Fig. 3A). Similar NMDA fractions of fEPSP were observed in WT and TgS slices under control conditions (Fig. 3B). Following removal of AMPA and NMDA blockade, LTP was induced and the NMDA fraction of fEPSP was re-determined 90 min later. WT, but not TgS, slices displayed predictably increased NMDAR component during the maintenance phase (Watt *et al.*, 2004; Fig. 3C, $n = 5$ of each, $P < 0.05$). These data suggest that overexpressed AChE-S interferes with the activity-dependent synaptic reorganization of both AMPA- and NMDA-mediated fEPSP.

Transgenic excess of inactive AChE induces LTP decay

ACh is known to function as a facilitatory modulator of LTP induction (Segal & Auerbach, 1997). Therefore, we tested if AChE-S contributes to the failing maintenance phase of LTP by facilitating ACh hydrolysis. To this end, we examined HFS–LTP in TgSIn mice, which overexpress the mutated human AChE-SIn carrying an insert of seven amino acids at the catalytic site. The insert abolishes the catalytic activity of AChE-SIn while maintaining its other biochemical features (Sternfeld *et al.*, 1998a,b; Fig. 4A). Hydrolytic AChE activity was significantly higher in TgS hippocampal homogenates, whereas TgSIn homogenates displayed lower activity levels than WT (Sternfeld *et al.*, 1998a,b; Fig. 4B). Next, we tested the expression of the AChE-S and -SIn transgenes in hippocampal neurons by labelling AChE mRNA with a cRNA probe directed against exon six, common to both AChE-S and AChE-SIn. *In situ* hybridization displayed, under similar exposure conditions, an apparent excess of AChE-S and -SIn transcripts in hippocampal slices from TgS and TgSIn as compared with WT brains (Fig. 4C). These findings suggest that inactive transgenic molecules partially replace the endogenous active variant in the TgSIn hippocampus. HFS–LTP in TgSIn slices displayed small, insignificantly higher levels of induction than TgS, reaching 239 ± 22% peak potentiation (Fig. 4D, $n = 11$ slices, six mice, the TgS traces from Fig. 1A are replotted against TgSIn). This potentiation diminished significantly at −21.9%/h, a similar rate to that of TgS slices, which declined to a level of 195 ± 9% within 2 h of induction ($P < 0.05$ as compared with WT). Therefore, under this stimulation protocol, excess AChE catalytic activity in the synapse appeared ineffective in LTP induction; rather, the common decay phenotype of HFS–LTP in TgS and TgSIn slices suggests involvement of non-enzymatic AChE activities. Non-hydrolytic roles of AChE were recently challenged (Cousin *et al.*, 2005), suggesting that all previously reported phenotypes can also be explained by the catalytic actions of AChE or ACh. However, our current findings suggest otherwise, compatible with a recent study where the TgS and TgSIn transgenes showed similar

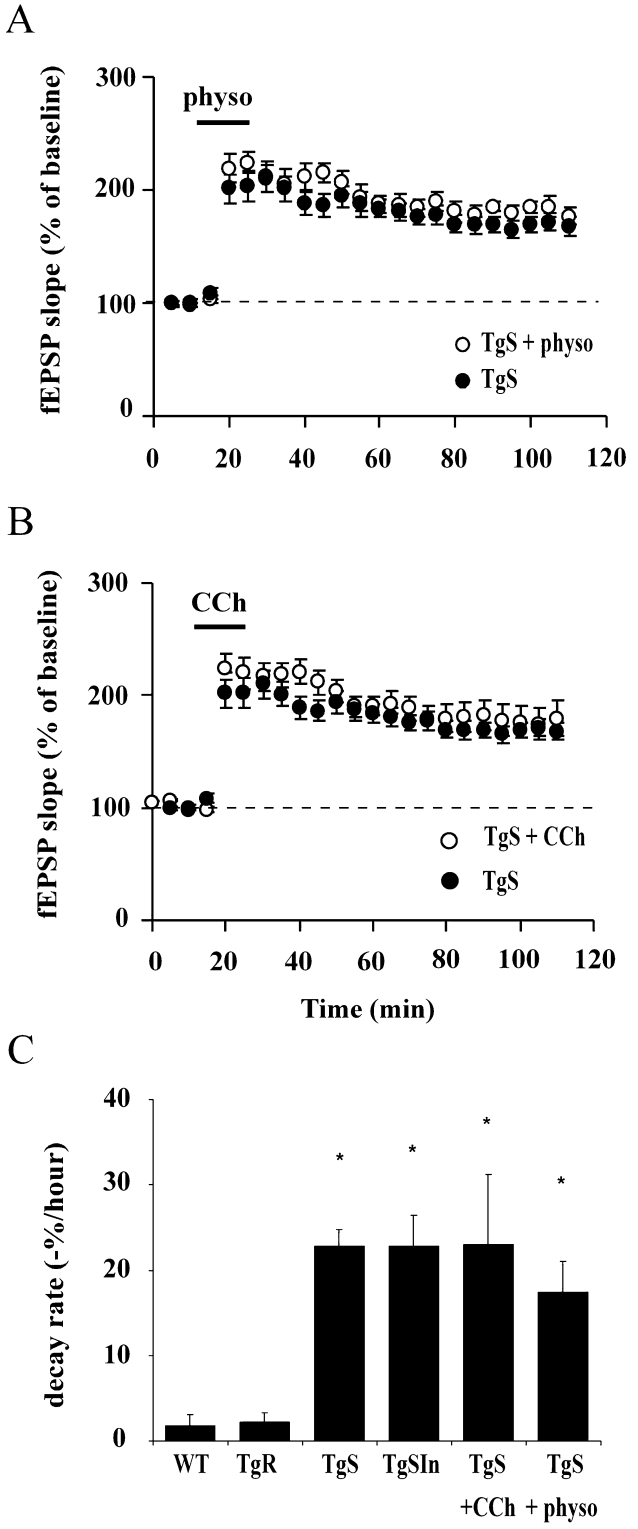

FIG. 5. The LTP decay involves AChE-S non-catalytic activities. Shown are LTP decaying patterns for hippocampal slices from TgS mice incubated 10 min before and 5 min after the induction phase with (A) physostigmine (physo, 1 μM) or (B) carbachol (CCh, 0.2 μM) as compared with untreated TgS slices (replotted from Fig. 1A). (C) Comparison of decay rates of TgS to the parallel patterns from WT, TgR or TgSIn mice. Decay rates were calculated as the percentage reduced potentiation at 90 min post-induction, where peak potentiation was set to 100%. *$P < 0.05$ compared to WT.

effects on the proliferation of neural progenitors in the developing murine brain (Dori *et al*., 2005).

Cholinergic activation fails to alleviate L-LTP in TgS mice

To challenge the hypothesis that non-enzymatic AChE activities were the cause for the impaired LTP maintenance, we induced hypercholinergic activation in the TgS slices. The carbamate AChE blocker, physostigmine (1 μM; Oh *et al*., 1999), served to block AChE catalytic activity, whereas the non-degradable ACh analogue, carbachol (CCh, 0.5 μM; Auerbach & Segal, 1994) was used to activate ACh receptors.

CCh and physostigmine application during the induction phase, 10 min before and 5 min after tetani, both induced small and insignificant increases in the level of TgS induction (19% and 17%, respectively), comparable to the 25% in WT slices under CCh treatment ($n = 6$ slices, four mice). Importantly, physostigmine application failed to rescue the maintenance phase in TgS slices, which closely followed the characteristic pattern of TgS LTP with 17.4%/h decay rate (from 219 ± 8% peak potentiation to 171 ± 9% 1.5 h post-tetanus, $n = 8$ slices, six mice, Fig. 5A, similar results for TgS slices are plotted). CCh administration also failed to rescue the maintenance phase, as was evident by the average 23%/h diminished potentiation observed during the 1.5 h post-tetanus (from 223 ± 12% peak potentiation to 179 ± 16%, $n = 11$ slices, eight mice, Fig. 5B, re-plotted results of TgS from Fig. 1A against TgS plus treatments). Averaged decay rates were compared from all animal models and experimental conditions, i.e. WT, TgR, TgS, TgSIn, TgS treated with CCh and TgS treated with physostigmine (Fig. 5C, $P < 0.05$). Decay rates were calculated as the percentage reduced potentiation during 90 min post-induction, where peak potentiation was normalized to 100%. The similar decay rates of the differently treated TgS slices thus contrasted the sustained potentiation in TgR and WT slices (Fig. 5C). That AChE activity levels were largely irrelevant strengthens the notion that the failure of LTP maintenance was due to the excess amount, not the catalytic activity, of AChE.

Impaired TgS transition to the LTP maintenance phase involves the PKC pathway

Next, we explored the putative biochemical signalling pathway(s) underlying the impaired transition to L-LTP. The adenylate cyclase activator, forskolin (50 μM) served to pharmacologically activate the cAMP/protein kinase A pathway, a necessary step for LTP stabilization (Matsushita *et al*., 2001). Forskolin induced in TgS slices a typical, slow-onset facilitation at the Schaffer collaterals–CA1 synapses. This facilitation closely tracked the potentiation development in WT slices (at 80 min from drug application, 191 ± 23% of baseline in TgS, $n = 5$ slices, four animals; 196 ± 20% of baseline in WT, $n = 6$ slices, four animals, Fig. 6A). Thus, excess AChE-S did not appear to alter the cAMP pathway reactions characteristic of L-LTP responses.

Excess AChE-R accumulation enables association with the protein kinase C (PKC) scaffold protein RACK1, which induces elevated PKCβII activity (Birikh *et al*., 2003). Compatible with this cascade, activation of PKC induced larger facilitation of TgR hippocampal synaptic potentials (Nijholt *et al*., 2004). This suggested an alternative signalling pathway, involving PKC in the elevated LTP response in TgR slices. Protein blots displayed reduction in PKCβII in TgS compared with WT hippocampi (Fig. 6B, $n = 7$ of each, $P < 0.05$). Impaired PKC activity or levels under dominance of AChE-S in TgS slices could potentially contribute to the impaired hippocampal HFS–LTP of TgS mice. To challenge this anticipation, we added the PKC

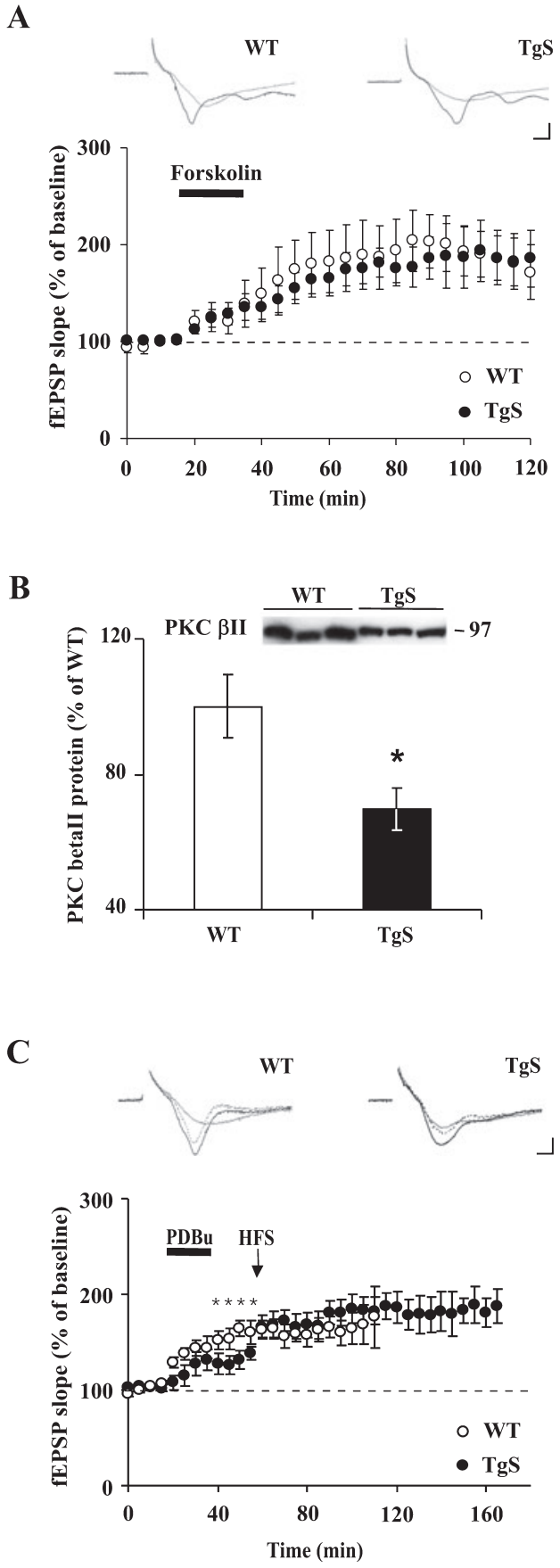

activator, PDBu (5 μM) to the treated slices. PDBu facilitated the fEPSP slope of TgS hippocampal slices only to 128 ± 5% of control, a significantly smaller increase than that of the WT slices response of 163 ± 8% (TgS, nine slices, six mice; WT, eight slices, six mice, $P < 0.03$, Fig. 7C). Tetanic stimulation yielded in TgS slices an additional potentiation that reached the PDBu-induced WT level (160 ± 12% in TgS, 164 ± 12% in WT, Fig. 6C), whereas PKC activation occluded HFS–LTP in WT slices. Moreover, when administered following PKC activation, tetanic stimulation rescued in TgS slices a stable potentiation pattern for up to 100 min. In conclusion, the failure to induce late-phase LTP in TgS mice was associated with reduced PKC amounts and activity. Therefore, at the biochemical level as well, AChE-R excess induced a PKC-mediated gain of function and AChE-S a loss of function, suggesting that the substitution of AChE-S with AChE-R is bimodally important for the stress-induced changes in LTP.

Transgenic AChE-S excess accentuates whereas AChE-R attenuates errors of performance in a serial choice maze

To explore the possible involvement of AChE alternative splicing in modulation of cognitive control under conflict conditions, we compared the maze performance of TgS, TgR and parental strain FVB/N mice. While fear conditioning can induce the 'freezing' motor response, and the cholinergic input to the hippocampus is required for fear-induced behavioural inhibition (Gray, 2000), errors of performance in general do not necessarily involve fear. Therefore, to avoid the confounding effect of fear (Birikh *et al*., 2003; Nijholt *et al*., 2004), we selected the use of a linear, two-choice maze in which a water-deprived mouse shuttles between the two ends of a straight one-lane maze to obtain a water reward (Quartermain *et al*., 1994). Preliminary experiments demonstrated that FVB/N mice could readily learn this maze. During the acquisition phase in which mice learn the path within the maze over the first 3 days, the incidence of errors progressively declined, in all three groups of mice (sessions S1–S3, Fig. 7). There were no statistically significant differences among the groups during acquisition, indicating comparable learning rates (Table 1). Over the subsequent 3 days (sessions S4–S6), termed 'the performance phase', we observed stable incidence of errors (Fig. 7B–E). However, during the performance phase, the groups differentiated, with TgS mice ($n = 11$) displaying more frequent performance errors compared with the parent strain FVB/N mice ($n = 14$), in contrast

FIG. 6. Excess AChE-S effects on synaptic plasticity engages the protein kinase C (PKC) cascade. Shown are the consequences of LTP induction field excitatory postsynaptic potential (fEPSP) facilitation values in hippocampal slices from wild-type (WT) and TgS mice under different treatment conditions. (A) Forskolin (50 μM) application elicits similar facilitation responses in TgS and WT slices, excluding protein kinase A involvement with the LTP differences. Also displayed are averaged samples of baseline (grey line) and forskolin-treated (black lines) fEPSPs from WT and TgS hippocampal slices, scales: 0.5 mV, 1.5 ms. (B) Reduced PKCβII levels in TgS hippocampal homogenates. Displayed are representative examples of immunoblotted PKCβII in three TgS and WT samples. Columns emphasize the significance of this difference. (C) Displayed are averaged samples of baseline (grey line), phorbol dibutyrate (PDBu; 5 μM)-treated (black dashed lines) and post-high-frequency stimulation (HFS; black lines) fEPSPs from WT and TgS hippocampal slices, scales: 0.5 mV, 1.5 ms. Below are averaged time courses of the fEPSP in response to PDBu application followed by HFS (arrow) in WT and TgS slices. PDBu induced a significantly smaller facilitation of the fEPSP slope of TgS slices as compared with WT. When followed by tetanic stimulation a significant increase was elicited in TgS, but none in WT. Note the stabilization of the LTP late phase in TgS. *$P < 0.05$ compared to WT.

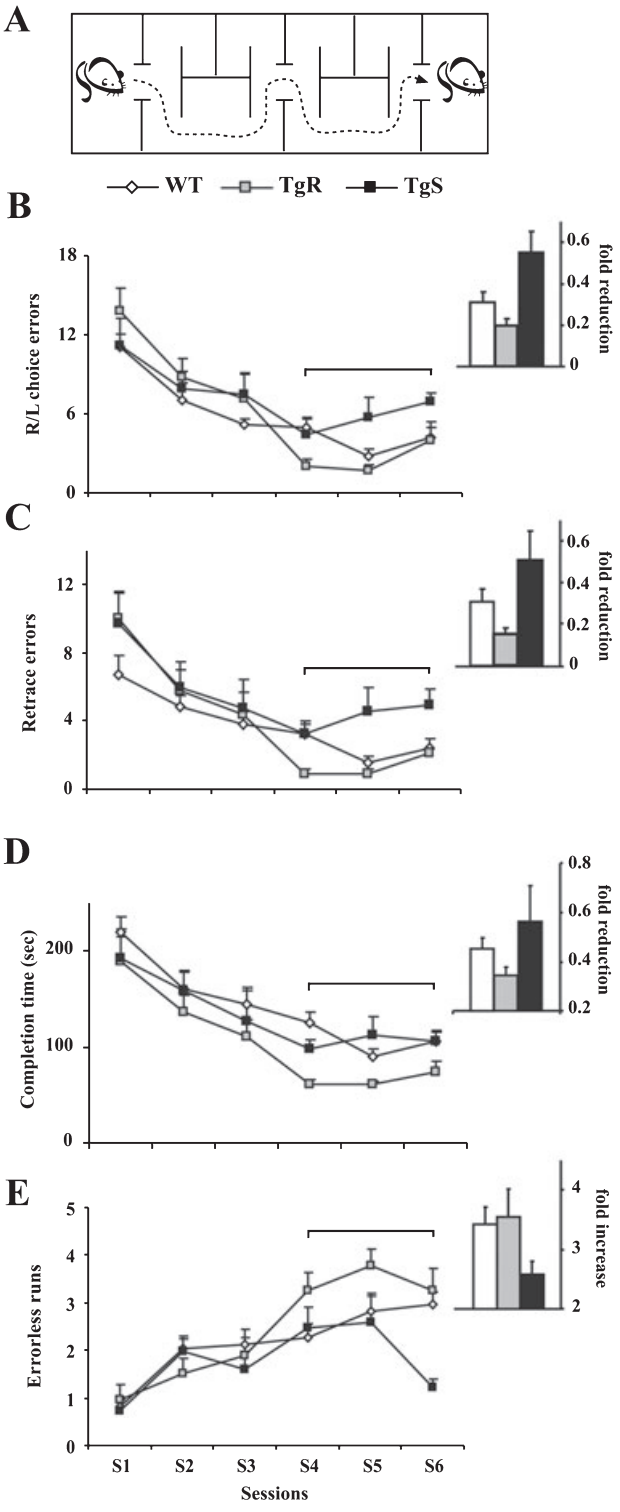

FIG. 7. Performance at a linear serial choice maze of transgenic excess of AChE-R (TgR), AChE-S (TgS) and wild-type FVB/N mice (WT). (A) Schematic presentation of the maze, each session included five successful runs. Shown is the averaged analysis of the number of right–left choice errors (B), retrace errors (C), the completion time of each session (D) and the total number of successful unidirectional runs (E). Note that in sessions S1–S3 performance was similar to all strains in all parameters, but in sessions S4–S6, the groups differentiated. The inset bar graph at (B–E) displays a fold reduction of averaged S5, S6 scores of the S1 score to demonstrate bidirectional, opposite effects of the TgS and TgR. See Table 1 for statistical analysis.

TABLE 1. Comparison of transgene effects in a serial choice maze

Analysis and measure	*F*-test	*Post hoc* N.K. tests
All six sessions		
R/L errors	N.S.	
Retrace errors	N.S.	
Completion time	$F_{2,30} = 4.94$; $P < 0.0139$	TgS, FVB > TgR
Errorless runs	$F_{2,30} = 3.13$; $P < 0.0581$	TgS < TgR
Last three sessions		
R/L errors	$F_{2,30} = 6.19$; $P < 0.0056$	TgS > FVB, TgR
Retrace errors	$F_{2,30} = 9.96$; $P < 0.0005$	TgS > FVB, TgR
Completion time	$F_{2,30} = 11.64$; $P < 0.0002$	TgS, FVB > TgR
Errorless runs	$F_{2,30} = 6.40$; $P < 0.0048$	TgS, FVB < TgR
Learning ratio (S5/S1%)		
R/L errors	$F_{2,30} = 5.92$; $P < 0.0068$	TgS < FVB, TgR
Retrace errors	$F_{2,30} = 4.18$; $P < 0.0250$	TgS < TgR
Completion time	$F_{2,30} = 3.15$; $P < 0.0571$	TgS < FVB, TgR

Analysis of variance with Newman–Keuls *post hoc* tests ($P < 0.05$) demonstrated improved learning ability with transgenic increase in AChE-R (TgR) and diminished learning ability with transgenic increase in AChE-S (TgS) compared with the native inbred line of FVB/N mice.

with fewer errors performed by TgR ($n = 8$) than FVB/N mice (see Table 1 for detailed statistical comparisons).

We have previously found neuromuscular alterations in TgS mice (Farchi *et al*., 2003). However, that study, unlike the current one, involved muscle strength measurements. In the serial maze, TgS mice showed no evidence of motor disability that could be the cause for their deficient maze performance, and all three mouse groups displayed similar completion times during the acquisition phase (Fig. 7D). The longer completion times displayed by TgS mice in the performance phase thus reliably reflected their greater number of errors. Most notable were TgS retrace errors (Fig. 7C). Namely, after reaching a deadend, TgS mice headed back to the position in which reward was no longer available. Hence, their significantly smaller number of errorless runs (Fig. 7E) might reflect both spatial orientation and executive function deficits. To assess the specificity of our data to cognitive performance, we further tested the transgenic mice in the elevated plus maze – a non-learning conflict situation (Trullas & Skolnick, 1993). Mice of all three groups displayed similar behavioural patterns in the elevated plus maze (Table 2). In a context where a response can not constitute an 'error', namely carry an adverse cost to the animal, alternative splicing of AChE is apparently not involved. This contrasts with the differential effect of transgene in the linear serial choice maze. AChE alternative splicing thus appears to remain involved with learning acquisition, but correlates with inverse direction of change in performance errors; increased for the maladaptive AChE-S and decreased for AChE-R.

Discussion

Alternative splicing is a key molecular process, modified under stress responses (Meshorer & Soreq, 2002; Stamm *et al*., 2005). However, exploring the adaptive value of splice variations remains a major task. Our present study explores the adaptive value of AChE splice site selection using transgenic overexpression of AChE splice variants. Transgenic overexpression of each splice variant creates conditions under which intrinsic splice selection is overshadowed by chronically elevated levels of the other splice variant. The impact of chronic overexpression of the AChE-S or AChE-R splice variants was

TABLE 2. Comparison of transgene effects in the elevated plus maze

Measure	FVB/N	TgS	TgR	*F*-test
Closed arm entries	14.6 ± 3.4	17.9 ± 4.9	18.0 ± 3.4	$F_{2,21} = 1.83$; $P < 0.1856$
Open arm entries	12.2 ± 2.0	13.9 ± 2.6	11.6 ± 2.8	$F_{2,21} = 1.71$; $P < 0.2045$
Total arm entries	26.9 ± 4.8	31.7 ± 5.2	29.6 ± 5.2	$F_{2,21} = 1.84$; $P < 0.1839$
Time in central square	83.2 ± 16.9	72.7 ± 23.2	75.6 ± 22.0	$F_{2,21} = 0.54$; $P < 0.5901$
Time in open arms	108.5 ± 30.0	107.0 ± 16.0	97.0 ± 34.0	$F_{2,21} = 0.40$; $P < 0.6722$
Head dip episodes	18.0 ± 5.6	22.6 ± 7.3	17.5 ± 11.5	$F_{2,21} = 0.88$; $P < 0.4276$

Analysis of variance revealed no differences among the transgenic lines TgS and TgR and the parental strain FVB/N.

explored at two levels of function related to cognition: synaptic hippocampal LTP and serial maze performance.

Mechanisms underlying LTP modulation by AChE alternative splicing

AChE-S overexpression led to diminished LTP induction and accelerated LTP decay compared with strain-matched FVB/N controls, whereas AChE-R overexpression led to stably enhanced LTP. A possible mechanism underlying these inverse effects may be morphological. TgS mice overexpressing the synapse-adhered human AChE-S exhibit progressively attenuated dendritic branching and accelerated spine loss (Beeri *et al*., 1997). Excess AChE-S but not AChE-R further induces morphological neuro-deterioration in the hippocampus (Sternfeld *et al*., 2000). These morphological features may be traced to altered neuronal gene expression (Meshorer *et al*., 2005a). The profile of gene expression in TgS mice includes changes in over 200 genes that can be expected to diminish LTP induction and L-LTP maintenance. In contrast, in TgR mice, excess AChE-R elevates the neuronal levels of the stress-induced splice factor SC35 (Meshorer *et al*., 2005b), which can be expected to globally affect neuronal gene expression.

In transgenic mice, we find that chronic AChE-R excess leads to an elevated HFS–LTP, suggesting that AChE-R is involved with facilitatory modulation of glutamatergic synaptic plasticity. Transgenic AChE-R excess induced a slower decay of TBS–LTP than that of WT slices, whereas excess AChE-S consistently exacerbated the decay phenotype of the LTP maintenance phase, even at HFS–LTP. These findings are compatible with the hypothesis that excess AChE acts separately on the maintenance and the induction phases. Moreover, our results suggest that alternative splicing contributes to the control mechanism(s) responsible for the transition to the LTP maintenance phase. Thus, adaptive and maladaptive splicing of AChE exerted inverse effects on LTP performance.

Importantly, neither the facilitatory nor the disruptive effects of AChE splice variants on LTP involve the catalytic properties of AChE. That excess of catalytically inactive AChE-SIn yielded a similar decay to that of AChE-S, and that cholinergic activation of TgS slices failed to rescue a normal phenotype, also attributes these actions of AChE to its non-catalytic properties. The similar LTP patterns of TgS and TgSIn slices and their contrast with TgR further weakens the possibility that the LTP decay is due to a position effect of these *ACHE* transgenes. The absence of strong cholinergic effects under excess catalytic AChE activity may be explained by the finding that hippocampal ACh levels are normal in awake TgS animals and lower only in anaesthetized ones, suggesting chronic overproduction of ACh that compensates for the synaptic AChE-S excess (Erb *et al*., 2001).

The electrotactin properties of AChE (Silman & Sussman, 2005) suggest that its non-catalytic capacities may compete with, and mediate, cell–cell and cell–matrix interactions. Neuroligin 1, for example, is a postsynaptic cell adhesion molecule of excitatory synapses (Chih *et al*., 2005), which includes an extracellular catalytically inactive AChE-homologous domain (Soreq & Seidman, 2001). When overexpressed, AChE-R may possibly compete with neuroligin for interaction with its partner protein β-neurexin (Nam & Chen, 2005). However, the distinct Ca^{2+} binding domains in AChE and neuroligin (Soreq & Seidman, 2001) predict differences in their adherence properties, suggesting that excess AChE-R may modify glutamatergic functions by impairing neurexin–neuroligin interactions.

The plasticity effects of AChE splice variants converge in the PKCβII response

Our findings suggest that AChE alternative splicing contributes to the control mechanism(s) responsible for the transition to the LTP maintenance phase in a manner converging in PKCβII expression in the hippocampal CA1 region. Apart from its extracellular function, AChE-R also accumulates intraneuronally, where it interacts with the scaffold protein RACK1 and its protein partner PKCβII (Birikh *et al*., 2003). This apparently modifies the capacity of RACK1 to regulate the IP3R pathway, which is intimately involved with LTP responses (Patterson *et al*., 2004). The AChE-R/RACK1/PKCβII interaction is catalytically independent (Perry *et al*., 2004) but physiologically effective, as is evident from the TgR/TgS different reactions to forskolin. Intriguingly, PKCβII is a stress-responsive splice variant of the PKCβ gene (Birikh *et al*., 2003), which determines the contextual fear response (Weeber *et al*., 2000). Together, the AChE and PKCβ splice modulations thus modify neuronal plasticity. In addition, others have recently shown that RACK1 brings PKC to the 40S ribosomal subunit, potentiating the phosphorylation of initiation factor 6, and thus exerting translational regulation under external stimuli (Nilsen, 2005). Competition by AChE-R on RACK1 interactions (Sklan *et al*., 2006) may cause general differences in translational processes under stress, facilitating the power of AChE splice site selection events.

Cognitive implications of alternative splicing effects

The bimodal differences in LTP performance between TgS and TgR mice raised the hypothesis that the AChE splice variants are bimodally involved in modulating learning performance as well. Furthermore, TgS mice display impaired learning and social recognition capacity (Cohen *et al*., 2002), and impaired spatial learning (Beeri *et al*., 1995). Indeed, in the present study, increased AChE-S production led to more errors in the serial choice paradigm. This effect, specific to the AChE-S transgene, was also specific to the learning situation, as no differences were detected among the mouse groups in the elevated plus maze. In

contrast, increased AChE-R production led to fewer errors in the serial choice paradigm. Several mechanisms may be considered.

Transgenic manipulations of the alternative splicing variants of AChE exerted inverse effects on performance. This enabled stress-independent assessment of the corresponding processes, exploring whether the replacement of AChE-S was an inert event, only required for producing AChE-R, or an evolutionarily conserved control mechanism that removes AChE-S for a reason, actively modulating the long-lasting adaptive neuronal stress responses. Our findings highlight a potentially important function for AChE-R in modulating of cognitive function. The capacity to produce AChE-R depends on one's age, gender, body mass index and ethnic origin, and contributes to trait and state anxiety parameters (Sklan *et al*., 2004). Malfunctioning under anxiety, for example in panic disorder patients (Battaglia & Ogliari, 2005), may hence be relevant to the inherited origin of splice site selection (Stamm *et al*., 2005). In addition, circulatory AChE-R determines the stress-induced changes in haematopoiesis (Grisaru *et al*., 2006), which also contributes to inflammatory reactions (Metz & Tracey, 2005). Brain–body communication thus depends largely on the splice site selection balance of AChE pre-mRNA transcripts (Pollak *et al*., 2005).

Cholinergic neurotransmission is notably associated with cognitive functions (Hirotsu *et al*., 1989; Blitzer *et al*., 1990; Ji *et al*., 2001; reviewed in Gold, 2003), responds to stress insults (Mark *et al*., 1996) and modifies LTP (Blitzer *et al*., 1990). Thus, differential effects of AChE-S vs. AChE-R overexpression on cholinergic pathways may underlie both physiological and behavioural performance differences observed here. However, brain AChE-R mapping (Sternfeld *et al*., 2000; Birikh *et al*., 2003) showed a transgenic increase of AChE-R both in neurons that are prime targets of cholinergic pathways and in brain regions that are not. Nevertheless, TgR mice displayed extensive numbers of AChE-R overexpressing neurons in the limbic cortex, especially the hippocampus and anterior cingulate cortex. Given the evidence for the role of these limbic cortical regions in monitoring errors of performance (Carter *et al*., 1998; McNaughton & Wickens, 2003), our current findings suggest that AChE-S is suppressed and AChE-R is recruited under stress in specific neural circuits that optimize LTP performance and decision-making processes under conditions of response competition. Further experiments will be required to find out whether the C-terminal peptide of AChE-S interacts with protein partner(s) explaining the consequent failure of cognitive response selection. Last, but not least, the effect of AChE inhibitors should be considered: patients with Alzheimer's disease receiving such treatment show elevated AChE-R levels (Darreh-Shori *et al*., 2004) associated with improved behaviour (Giacobini, 2003a,b), which may reflect parallel processes to those described in this study.

Acknowledgements

This study was supported by the Israel Science Fund (Grants 618y02 and 484/02 to H.S. and S.S.), the European Community (LSHM-CT-2003-503330, LSH-2004-1.1.5-3 to H.S.) and by Ester Neuroscience, Ltd (Tel. Aviv).

Abbreviations

AChE, acetylcholinesterase; ACSF, artificial cerebrospinal fluid; AMPAR, α-amino-3-hydroxy-5-methylisoxazole-4-propionate receptor; CCh, carbachol; DMSO, dimethylsulphoxide; fEPSP, field excitatory postsynaptic potentials; HFS, high-frequency stimulation; LTP, long-term potentiation; NMDAR, *N*-methyl-D-aspartate receptor; PDBu, phorbol dibutyrate; PKC, protein kinase C; RACK1, receptor of activated C kinase 1; TBS, theta burst stimulation; Tg, transgenic; WT, wild-type.

References

al'Absi, M., Hugdahl, K. & Lovallo, W.R. (2002) Adrenocortical stress responses and altered working memory performance. *Psychophysiology*, **39**, 95–99.

Aigner, T.G. (1995) Pharmacology of memory: cholinergic–glutamatergic interactions. *Curr. Opin. Neurobiol.*, **5**, 155–160.

Auerbach, J.M. & Segal, M. (1994) A novel cholinergic induction of long-term potentiation in rat hippocampus. *J. Neurophysiol.*, **72**, 2034–2040.

Battaglia, M. & Ogliari, A. (2005) Anxiety and panic: from human studies to animal research and back. *Neurosci. Biobehav. Rev.*, **29**, 169–179.

Beeri, R., Andres, C., Lev-Lehman, E., Timberg, R., Huberman, T., Shani, M. & Soreq, H. (1995) Transgenic expression of human acetylcholinesterase induces progressive cognitive deterioration in mice. *Curr. Biol.*, **5**, 1063–1071.

Beeri, R., Le Novere, N., Mervis, R., Huberman, T., Grauer, E., Changeux, J.P. & Soreq, H. (1997) Enhanced hemicholinium binding and attenuated dendrite branching in cognitively impaired acetylcholinesterase-transgenic mice. *J. Neurochem.*, **69**, 2441–2451.

Birikh, K., Sklan, E., Shoham, S. & Soreq, H. (2003) Interaction of 'readthrough' acetylcholinesterase with RACK1 and PKCbetaII correlates with intensified fear-induced conflict behavior. *Proc. Natl Acad. Sci. USA*, **100**, 283–288.

Blank, T., Nijholt, I., Eckart, K. & Spiess, J. (2002) Priming of long-term potentiation in mouse hippocampus by corticotropin-releasing factor and acute stress: implications for hippocampus-dependent learning. *J. Neurosci.*, **22**, 3788–3794.

Blitzer, R.D., Gil, O. & Landau, E.M. (1990) Cholinergic stimulation enhances long-term potentiation in the CA1 region of rat hippocampus. *Neurosci. Lett.*, **119**, 207–210.

Carter, C.S., Braver, T.S., Barch, D.M., Botvinick, M.M., Noll, D. & Cohen, J.D. (1998) Anterior cingulate cortex, error detection, and the online monitoring of performance. *Science*, **280**, 747–749.

Chih, B., Engelman, H. & Scheiffele, P. (2005) Control of excitatory and inhibitory synapse formation by neuroligins. *Science*, **307**, 1324–1328.

Cohen, O., Erb, C., Ginzberg, D., Pollak, Y., Seidman, S., Shoham, S., Yirmiya, R. & Soreq, H. (2002) Neuronal overexpression of 'readthrough' acetylcholinesterase is associated with antisense-suppressible behavioral impairments. *Mol. Psychiatry*, **7**, 874–885.

Cousin, X., Strahle, U. & Chatonnet, A. (2005) Are there non-catalytic functions of acetylcholinesterases? Lessons from mutant animal models. *Bioessays*, **27**, 189–200.

Darreh-Shori, T., Hellstrom-Lindahl, E., Flores-Flores, C., Guan, Z.Z., Soreq, H. & Nordberg, A. (2004) Long-lasting acetylcholinesterase splice variations in anticholinesterase-treated Alzheimer's disease patients. *J. Neurochem.*, **88**, 1102–1113.

Diamond, D.M., Park, C.R., Heman, K.L. & Rose, G.M. (1999) Exposing rats to a predator impairs spatial working memory in the radial arm water maze. *Hippocampus*, **9**, 542–552.

Dori, A., Cohen, J., Silverman, W.F., Pollack, Y. & Soreq, H. (2005) Functional manipulations of acetylcholinesterase splice variants highlight alternative splicing contributions to murine neocortical development. *Cereb. Cortex*, **15**, 419–430.

Ellman, G.L., Courtney, D., Andres, V.J. & Featherstone, R.M. (1961) A new and rapid colorimetric determination of acetylcholinesterase activity. *Biochem. Pharmacol.*, **7**, 88–95.

Erb, C., Troost, J., Kopf, S., Schmitt, U., Loffelholz, K., Soreq, H. & Klein, J. (2001) Compensatory mechanisms enhance hippocampal acetylcholine release in transgenic mice expressing human acetylcholinesterase. *J. Neurochem.*, **77**, 638–646.

Farchi, N., Soreq, H. & Hochner, B. (2003) Chronic acetylcholinesterase overexpression induces multilevelled aberrations in mouse neuromuscular physiology. *J. Physiol.*, **546**, 165–173.

Foy, M.R., Stanton, M.E., Levine, S. & Thompson, R.F. (1987) Behavioral stress impairs long-term potentiation in rodent hippocampus. *Behav. Neural Biol.*, **48**, 138–149.

Giacobini, E. (2003a) Cholinergic function and Alzheimer's disease. *Int. J. Geriatr. Psychiatry*, **18**, S1–S5.

Giacobini, E. (2003b) Cholinesterases: new roles in brain function and in Alzheimer's disease. *Neurochem. Res.*, **28**, 515–522.

Gold, P.E. (2003) Acetylcholine modulation of neural systems involved in learning and memory. *Neurobiol. Learn. Mem.*, **80**, 194–210.

Gray, J.A. (2000) *The Neuropsychology of Anxiety: an Inquiry into the Functions of the Septo-Hippocampal System*. Oxford University Press, Oxford, UK.

Grisaru, D., Pick, M., Perry, C., Sklan, E.H., Almog, R., Goldberg, I., Naparstek, E., Lessing, J.B., Soreq, H. & Deutsch, V. (2006) Hydrolytic and nonenzymatic functions of acetylcholinesterase comodulate hemopoietic stress responses. *J. Immunol.*, **176**, 27–35.

Hirotsu, I., Hori, N., Katsuda, N. & Ishihara, T. (1989) Effect of anticholinergic drug on long-term potentiation in rat hippocampal slices. *Brain Res.*, **482**, 194–197.

Hochner, B., Parnas, H. & Parnas, I. (1991) Effects of intra-axonal injection of Ca2+ buffers on evoked release and on facilitation in the crayfish neuromuscular junction. *Neurosci. Lett.*, **125**, 215–218.

Ji, D., Lape, R. & Dani, J.A. (2001) Timing and location of nicotinic activity enhances or depresses hippocampal synaptic plasticity. *Neuron*, **31**, 131–141.

Kaufer, D., Friedman, A., Seidman, S. & Soreq, H. (1998) Acute stress facilitates long-lasting changes in cholinergic gene expression. *Nature*, **393**, 373–377.

Kim, J.J. & Diamond, D.M. (2002) The stressed hippocampus, synaptic plasticity and lost memories. *Nat. Rev. Neurosci.*, **3**, 453–462.

Mark, G.P., Rada, P.V. & Shors, T.J. (1996) Inescapable stress enhances extracellular acetylcholine in the rat hippocampus and prefrontal cortex but not the nucleus accumbens or amygdala. *Neuroscience*, **74**, 767–774.

Maskos, U., Molles, B.E., Pons, S., Besson, M., Guiard, B.P., Guilloux, J.P., Evrard, A., Cazala, P., Cormier, A., Mameli-Engvall, M., Dufour, N., Cloez-Tayarani, I., Bemelmans, A.P., Mallet, J., Gardier, A.M., David, V., Faure, P., Granon, S. & Changeux, J.P. (2005) Nicotine reinforcement and cognition restored by targeted expression of nicotinic receptors. *Nature*, **436**, 103–107.

Matsushita, M., Tomizawa, K., Moriwaki, A., Li, S.T., Terada, H. & Matsui, H. (2001) A high-efficiency protein transduction system demonstrating the role of PKA in long-lasting long-term potentiation. *J. Neurosci.*, **21**, 6000–6007.

McNaughton, N. & Wickens, J. (2003) Hebb, pandemonium and catastrophic hypermnesia: the hippocampus as a suppressor of inappropriate associations. *Cortex*, **39**, 1139–1163.

Meshorer, E., Biton, I.E., Ben-Shaul, Y., Ben-Ari, S., Assaf, Y., Soreq, H. & Cohen, Y. (2005a) Chronic cholinergic imbalances promote brain diffusion and transport abnormalities. *Faseb J.*, **19**, 910–922.

Meshorer, E., Bryk, B., Toiber, D., Cohen, J., Podoly, E., Dori, A. & Soreq, H. (2005b) SC35 promotes sustainable stress-induced alternative splicing of neuronal acetylcholinesterase mRNA. *Mol. Psychiatry*, **10**, 985–997.

Meshorer, E., Erb, C., Gazit, R., Pavlovsky, L., Kaufer, D., Friedman, A., Glick, D., Ben-Arie, N. & Soreq, H. (2002) Alternative splicing and neuritic mRNA translocation under long-term neuronal hypersensitivity. *Science*, **295**, 508–512.

Meshorer, E. & Soreq, H. (2002) Pre-mRNA splicing modulations in senescence. *Ageing Cell*, **1**, 6–10.

Meshorer, E. & Soreq, H. (2006) Alternative AChE splice variants in stress-related neuropathologies. *Trends Neurosci.*, **29**, 216–224.

Metz, C.N. & Tracey, K.J. (2005) It takes nerve to dampen inflammation. *Nat. Immunol.*, **6**, 756–757.

Mineur, Y.S. & Crusio, W.E. (2002) Behavioral and neuroanatomical characterization of FVB/N inbred mice. *Brain Res. Bull.*, **57**, 41–47.

Nam, C.I. & Chen, L. (2005) Postsynaptic assembly induced by neurexin–neuroligin interaction and neurotransmitter. *Proc. Natl Acad. Sci. USA*, **102**, 6137–6142.

Nijholt, I., Farchi, N., Kye, M., Sklan, E.H., Shoham, S., Verbeure, B., Owen, D., Hochner, B., Spiess, J., Soreq, H. & Blank, T. (2004) Stress-induced alternative splicing of acetylcholinesterase results in enhanced fear memory and long-term potentiation. *Mol. Psychiatry*, **9**, 174–183.

Nilsen, T.W. (2005) Spliceosome assembly in yeast: one ChIP at a time? *Nat. Struct. Mol. Biol.*, **12**, 571–573.

Oh, M.M., Power, J.M., Thompson, L.T., Moriearty, P.L. & Disterhoft, J.F. (1999) Metrifonate increases neuronal excitability in CA1 pyramidal neurons from both young and aging rabbit hippocampus. *J. Neurosci.*, **19**, 1814–1823.

Patterson, R.L., van Rossum, D.B., Barrow, R.K. & Snyder, S.H. (2004) RACK1 binds to inositol 1,4,5-trisphosphate receptors and mediates Ca2+ release. *Proc. Natl Acad. Sci. USA*, **101**, 2328–2332.

Perrier, N.A., Salani, M., Falasca, C., Bon, S., Augusti-Tocco, G. & Massoulie, J. (2005) The readthrough variant of acetylcholinesterase remains very minor after heat shock, organophosphate inhibition and stress, in cell culture and in vivo. *J. Neurochem.*, **94**, 629–638.

Perry, C., Sklan, E.H. & Soreq, H. (2004) CREB regulates AChE-R-induced proliferation of human glioblastoma cells. *Neoplasia*, **6**, 279–286.

Pollak, Y., Gilboa, A., Ben-Menachem., O., Ben-Hur, T., Soreq, H. & Yirmiya, R. (2005) Acetylcholinesterase inhibitors reduce brain and blood interleukin-1beta production. *Ann. Neurol.*, **57**, 741–745.

Quartermain, D., Mower, J., Rafferty, M.F., Herting, R.L. & Lanthorn, T.H. (1994) Acute but not chronic activation of the NMDA-coupled glycine receptor with D-cycloserine facilitates learning and retention. *Eur. J. Pharmacol.*, **257**, 7–12.

Royle, S.J., Collins, F.C., Rupniak, H.T., Barnes, J.C. & Anderson, R. (1999) Behavioural analysis and susceptibility to CNS injury of four inbred strains of mice. *Brain Res.*, **816**, 337–349.

Sapolsky, R. (2003) Bugs in the brain. *Sci. Am.*, **288**, 94–97.

Segal, M. & Auerbach, J.M. (1997) Muscarinic receptors involved in hippocampal plasticity. *Life Sci.*, **60**, 1085–1091.

Shin, C. & Manley, J.L. (2004) Cell signalling and the control of pre-mRNA splicing. *Nat. Rev. Mol. Cell Biol.*, **5**, 727–738.

Shors, T.J., Seib, T.B., Levine, S. & Thompson, R.F. (1989) Inescapable versus escapable shock modulates long-term potentiation in the rat hippocampus. *Science*, **244**, 224–226.

Silman, I. & Sussman, J.L. (2005) Acetylcholinesterase: 'classical' and 'non-classical' functions and pharmacology. *Curr. Opin. Pharmacol.*, **5**, 293–302.

Sklan, E.H., Lowenthal, A., Korner, M., Ritov, Y., Landers, D.M., Rankinen, T., Bouchard, C., Leon, A.S., Rice, T., Rao, D.C., Wilmore, J.H., Skinner, J.S. & Soreq, H. (2004) Acetylcholinesterase/paraoxonase genotype and expression predict anxiety scores in Health, Risk Factors, Exercise Training, and Genetics study. *Proc. Natl Acad. Sci. USA*, **101**, 5512–5517.

Sklan, E.H., Podoly, E. & Soreq, H. (2006) RACK1 has the nerve to act: structure meets function in the nervous system. *Prog. Neurobiol.*, **78**, 117–134.

Sokolov, M.V. & Kleschevnikov, A.M. (1995) Atropine suppresses associative LTP in the CA1 region of rat hippocampal slices. *Brain Res.*, **672**, 281–284.

Soreq, H. & Seidman, S. (2001) Acetylcholinesterase – new roles for an old actor. *Nat. Rev. Neurosci.*, **2**, 294–302.

Stamm, S., Ben-Ari, S., Rafalska, I., Tang, Y., Zhang, Z., Toiber, D., Thanaraj, T.A. & Soreq, H. (2005) Function of alternative splicing. *Gene*, **344**, 1–20.

Sternfeld, M., Ming, G., Song, H., Sela, K., Timberg, R., Poo, M. & Soreq, H. (1998a) Acetylcholinesterase enhances neurite growth and synapse development through alternative contributions of its hydrolytic capacity, core protein, and variable C termini. *J. Neurosci.*, **18**, 1240–1249.

Sternfeld, M., Patrick, J.D. & Soreq, H. (1998b) Position effect variegations and brain-specific silencing in transgenic mice overexpressing human acetylcholinesterase variants. *J. Physiol. Paris*, **92**, 249–255.

Sternfeld, M., Shoham, S., Klein, O., Flores-Flores, C., Evron, T., Idelson, G.H., Kitsberg, D., Patrick, J.W. & Soreq, H. (2000) Excess 'readthrough' acetylcholinesterase attenuates but the 'synaptic' variant intensifies neurodeterioration correlates. *Proc. Natl. Acad. Sci. USA*, **97**, 8647–8652.

Stoilov, P., Meshorer, E., Gencheva, M., Glick, D., Soreq, H. & Stamm, S. (2002) Defects in pre-mRNA processing as causes of and predisposition to diseases. *DNA Cell Biol.*, **21**, 803–818.

Trullas, R. & Skolnick, P. (1993) Differences in fear motivated behaviors among inbred mouse strains. *Psychopharmacology (Berl.)*, **111**, 323–331.

Watt, A.J., Sjostrom, P.J., Hausser, M., Nelson, S.B. & Turrigiano, G.G. (2004) A proportional but slower NMDA potentiation follows AMPA potentiation in LTP. *Nat. Neurosci.*, **7**, 518–524.

Weeber, E.J., Atkins, C.M., Selcher, J.C., Varga, A.W., Mirnikjoo, B., Paylor, R., Leitges, M. & Sweatt, J.D. (2000) A role for the beta isoform of protein kinase C in fear conditioning. *J. Neurosci.*, **20**, 5906–5914.